Temperature dependence of coherent A 1 g and E g phonons of bismuth

Kunie Ishioka, Masahiro Kitajima, and Oleg V. Misochko

Citation: Journal of Applied Physics **100**, 093501 (2006); doi: 10.1063/1.2363746
View online: http://dx.doi.org/10.1063/1.2363746
View Table of Contents: http://scitation.aip.org/content/aip/journal/jap/100/9?ver=pdfcov
Published by the AIP Publishing

Temperature dependence of coherent A_{1g} and E_g phonons of bismuth

Kunie Ishioka[a)]
Advanced Nano-Characterization Center, National Institute for Materials Science, Tsukuba 305-0047, Japan

Masahiro Kitajima
Advanced Nano-Characterization Center, National Institute for Materials Science, Tsukuba 305-0047, Japan

Oleg V. Misochko
Institute of Solid State Physics, Russian Academy of Sciences, 142432 Chernogolovka, Moscow, Russia

(Received 16 April 2006; accepted 1 August 2006; published online 1 November 2006)

Bismuth has been a model material in the study of femtosecond dynamics of coherent lattice oscillations. The generation mechanism was first proposed to be displacive for the symmetric A_{1g} mode, which was the only mode observed as a coherent phonon. The absence of the other Raman active mode E_g has not been fully explained, but was phenomenologically attributed to the exclusive coupling of the hot electrons at $k \sim 0$ and high symmetry phonons. In the present study, we demonstrate that both A_{1g} and E_g modes are excited as coherent phonons at low temperature and confirm that the coherent phonons are generated via a Raman process in bismuth. We found a puzzling $\pi/2$ difference in the initial phases of the two coherent phonons, which suggests that the initial phase cannot be a clear-cut index for the generation mechanism in absorbing media. © *2006 American Institute of Physics*. [DOI: 10.1063/1.2363746]

I. INTRODUCTION

Irradiation of ultrashort optical pulses on solids impulsively induces, among other elementary excitations, coherent optical phonons.[1,2] They are observed as the oscillating changes in the optical properties in picosecond to femtosecond time scale and are coherent in the sense that two optical pulses, time separated but not phase locked, can enhance or destroy the oscillation depending on the separation between the pulses.[3] Up to now, it is almost exclusively the Raman active modes that have been observed as coherent phonons. The selection rule has been explained on the basis of Raman processes included both in the generation and detection.[1,2]

For the detection, the refractive index n and the susceptibility χ is modulated according to the nuclear displacement Q. The modulation in optical properties such as reflectivity R and transmittance T is therefore approximately proportional to Q,

$$\Delta R = \frac{\partial R}{\partial n}\Delta n \approx \frac{\partial R}{\partial \chi}\frac{\partial \chi}{\partial Q}Q, \tag{1}$$

which makes ΔR (and ΔT) a quantitative, though not absolute, measure for Q. Because $(\partial\chi)/(\partial Q)$ is a first-order Raman tensor, only Raman active modes have nonzero $(\partial\chi)/(\partial Q)$ and can be detected as a modulation in optical properties.

For the generation, a short optical pulse with a broad spectrum can induce a stimulated Raman process to excite impulsively Raman active phonons.[1] This impulsive stimulated Raman scattering (ISRS) is the only known generation mechanism for transparent materials. The nuclear oscillations are considered to be on the ground electronic states, and the initial phase δ of the oscillation to be zero when fitted to $\exp(-\Gamma t)\sin(2\pi\nu t+\delta)$. In absorbing materials, other generation mechanisms related to photoexcited carrier dynamics have been widely accepted, in addition to the ISRS process. They are driven by the sudden screening of the surface field or the photo-Dember effect and are restricted to certain types of semiconductors.[2] It is possible to excite Raman inactive modes as coherent phonons in such semiconductors and detect them by means of a nonoptical technique, e.g., terahertz emission.

On the other hand, some Raman active modes failed to be observed as coherent phonons, even with short enough optical pulses. One such example is the E_g mode of bismuth (Bi). Bi has two Raman active phonons with second rank Raman tensors,

$$A_{1g} = \begin{pmatrix} a & 0 & 0 \\ 0 & a & 0 \\ 0 & 0 & b \end{pmatrix} \tag{2}$$

and

$$E_g = \begin{pmatrix} c & 0 & 0 \\ 0 & -c & d \\ 0 & d & 0 \end{pmatrix} \quad \text{or} \quad \begin{pmatrix} 0 & -c & -d \\ -c & 0 & 0 \\ -d & 0 & 0 \end{pmatrix}. \tag{3}$$

at frequencies of 2.9 and 2.2 THz, respectively.[4,5] Early pump-probe experiments reported the coherent A_{1g} phonon, but failed to observe the coherent E_g phonon.[6–8] A later experiment found the coherent E_g phonon after deleting much stronger A_{1g} component by polarization analysis,[3] yet the relative intensity was considerably smaller than that in spontaneous Raman studies. The "absence" of the E_g mode, together with the initial phase $\delta \sim \pi/2$ of the A_{1g} mode,[8–10] lead the previous authors to an alternative generation mechanism of displacive excitation of coherent phonon (DECP), in which a sudden shift of the vibrational potential at photoex-

[a)]Electronic mail: ishioka.kunie@nims.go.jp

citation kick-starts the coherent oscillation on the electronic excited state. The absence of the E_g mode was tentatively explained in terms of an exclusive coupling of photoexcited electrons at $k \sim 0$ with the fully symmetric (A_{1g}) phonon, yet no explanation was given as to why the coupling should be exclusive. A later theoretical study rendered the DECP a resonant case of the ISRS,[11] which made the absence of the Raman active E_g mode even more puzzling.

Recent experimental studies have revealed peculiar behaviors of the coherent phonons of Bi under intense photoexcitatoin. The A_{1g} mode showed a time-dependent frequency shift, whose origin is under heated debate.[12–14] The coherent E_g phonon became visible without polarization analysis.[12] Under even more intense excitation, the coherent phonons exhibited an amplitude collapse-revival,[15] which cannot be described within the frame of classical mechanics. However, the lattice dynamics under moderate photoexcitation, on which the discussion on the above anomalies should be based, leaves many unsolved questions to date.

In the present study, we investigate the ultrafast dynamics of the coherent phonons of single crystal Bi under moderate photoexcitation as a function of temperature, excitation density, and optical polarization. We demonstrate that both of the two Ramanactive modes are excited as coherent phonons via resonant ISRS at low temperature. Coherent E_g phonon vanishes more rapidly than A_{1g} with rising temperature, possibly because of its larger coupling with lower-frequency phonons. We find that the initial phases of the two phonons are shifted from each other and propose an explanation in terms of the vibrational potential on the excited state.

II. EXPERIMENT

Single crystal Bi with surfaces perpendicular to the trigonal axis [0001] are mounted in a closed-cycle cryostat, with its $[11\bar{2}0]$ axis in vertical direction. Pump-probe reflectivity measurements are performed using optical pulses with 60 fs duration, 800 nm wavelength, and 86 MHz repetition rate. A plano-convex lens brings the linearly polarized pump and probe beams to a 30 μm focus on the sample with angles of $<5°$ and 15° from the surface normal, respectively. Pump and probe powers are kept at 5 and 1 mW (pulse energies of 9.3 and 1.9 $\mu J/cm^2$), respectively to prevent laser-induced heating, except for the pump-power dependence measurements. Pump beam is modulated at 1.98 kHz with an optical chopper for lock-in detection. Time delay t between the pump and probe pulses is scanned by a translational stage (slow scan) to enable a precise estimation of the reflectivity change and a scan over several tens of picoseconds of delay time.

For isotropic reflectivity measurements, the incident probe beam is horizontally polarized (p polarization), and its p component is detected with a p-i-n detector after reflection from the sample. The difference between the signal (probe after the sample) and the reference (before the sample) is preamplified and recorded to cancel the fluctuation in the laser power and to enable an amplification of the small change in the reflectivity (typically $\Delta R/R \sim 10^{-6}$). For anisotropic reflectivity measurements, the incident probe beam is polarized 45° with respect to the optical plane. After reflection from the sample, the probe beam is analyzed into s- and p-polarized components and detected with matched photodiodes [electro-optic (EO) sampling]. By taking the difference between the two photocurrents $\Delta R_{EO} = \Delta R_p - \Delta R_s$, we eliminate the isotropic response of the A_{1g} phonon and photoexcited electrons in order to record the weaker anisotropic signal of the E_g phonon.

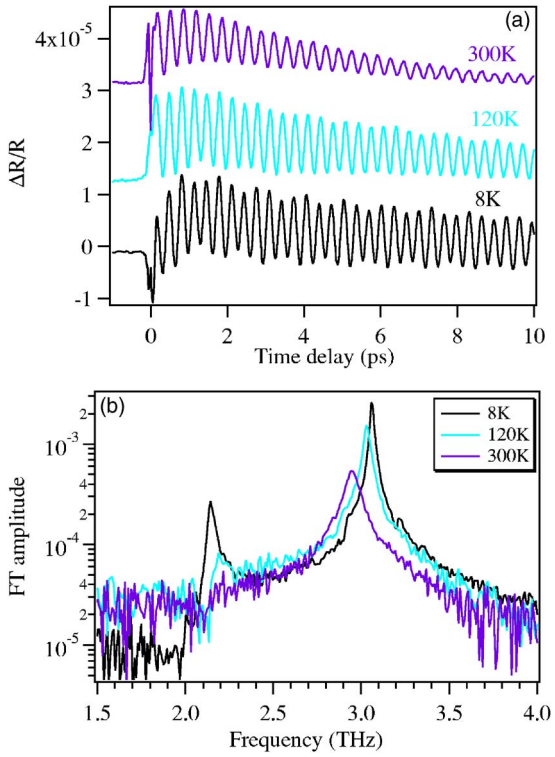

FIG. 1. (Color online) (a) Isotropic reflectivity change $\Delta R/R$ of Bi under 5 mW excitation and (b) its Fourier transform (FT) spectra at different temperatures. Pump and probe beams are s and p polarized, respectively. Traces in (a) are offset for clarity.

III. RESULTS

A. Temperature dependence

Transient isotropic reflectivity change of Bi consists of nonoscillatory (electronic) and oscillatory (phononic) contributions, as shown in Fig. 1(a). At room temperature, the oscillatory part is fitted to a single damped harmonic oscillation due to the coherent A_{1g} phonon.[6–8] Correspondingly, Fourier transformed (FT) spectrum is dominated by a single peak at 2.95 THz, as shown in Fig. 1(b). On lowering temperature, the oscillation in the reflectivity is modulated to show a beating pattern. It is induced by the appearance of another coherent oscillation at ~2.15 THz, as shown clearly in Fig. 1(b), which is attributed to the coherent E_g phonon.[3] Anisotropic reflectivity change reveals the behavior of the E_g phonon more clearly, as shown in Fig. 2, since the isotropic A_{1g} mode is canceled in this detection scheme. While no oscillation is detected in the reflectivity at room temperature, the coherent E_g phonon becomes visible on lowering temperature. The appearance of a small A_{1g} component is due to polarization leakage. We note that the E_g amplitude (or peak

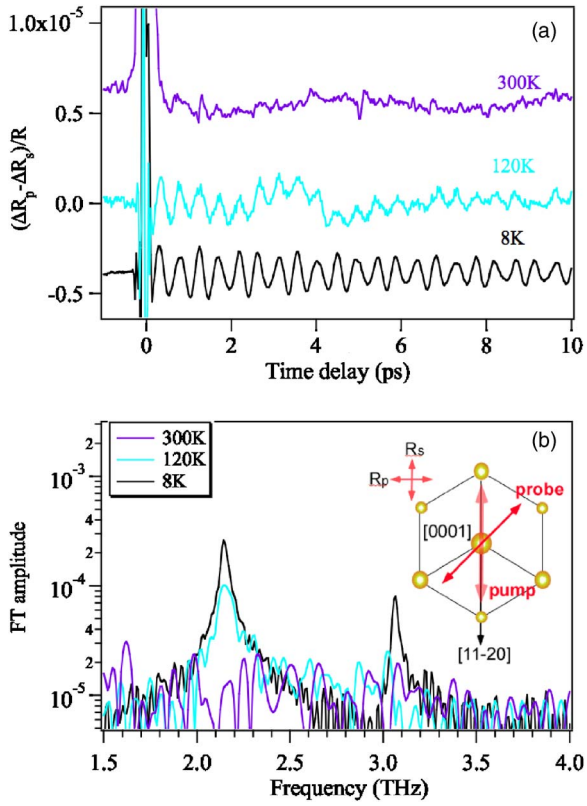

FIG. 2. (Color online) (a) Anisotropic reflectivity change $\Delta R_{EO}/R$ of Bi under 5 mW excitation, and (b) its FT spectra, at different temperatures. Inset in (b) shows the polarization configuration of the anisotroic measurements superimposed on the (0001) plane of Bi.

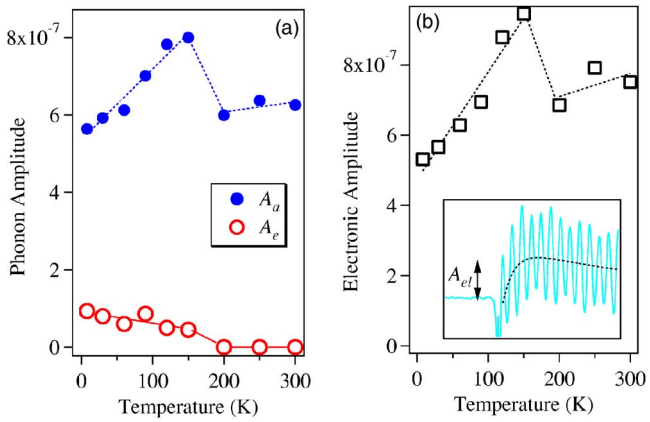

FIG. 3. (Color online) Temperature dependence of (a) the initial amplitudes A_a and A_e of coherent A_{1g} and E_g phonons of Bi and (b) the amplitude of the electronic transient A_{el}. Lines are to guide the eyes. Inset in (b) illustrates how to obtain A_{el} as the maximum height of the nonoscillatory part (dotted curve) of the isotropic reflectivity change.

height) obtained from the anisotropic measurement agrees with that from the isotropic measurement within an experimental error. Our observation gives a clear counterevidence against the empirical selection rule for the fully symmetric phonons in the framework of DECP,[8] and confirms that all the Raman active modes can be excited as coherent phonons.

The absence of the E_g phonon at room temperature appears to contradict the preceding time-domain study, where the coherent E_g phonon was observed in anisotropic reflectivity measurement.[3] We attribute the discrepancy to different sample orientations. The previous study used polycrystalline film as the sample and therefore probed nonbasal planes as well as basal planes. We speculate that the Raman tensor element d for the nonbasal plane is much larger than c for the basal plane, and thus contributed to the room temperature observation in the previous study. Another factor is that single crystal Bi is much more sensitive to laser-induced damage than polycrystalline at room temperature. We will show in Sec. III C that laser irradiation at room temperature can easily melt single crystal Bi and recrystallize at random crystallographic orientations. The oscillatory part of the reflectivity change for $t>0$ is fitted to a double damped harmonic function,

$$f(t) = A_a \exp(-\Gamma_a t)\sin(2\pi\nu_a t + \delta_a) + A_e \exp(-\Gamma_e t)\sin(2\pi\nu_e t + \delta_e). \quad (4)$$

Here subscripts a and e denote A_{1g} and E_g phonons, respectively. According to Eq. (1), the amplitudes in the reflectivity, A_a and A_e, are approximately proportional to the nuclear displacement Q in the real space, and one can therefore regard them as quantitative measure for Q. Figure 3(a) clearly demonstrates that a coherent E_g phonon is generated (i.e., $A_e \neq 0$) only below 200 K. A_e decreases slightly with rising temperature and drops abruptly to zero between 150 and 200 K. Temperature dependence of A_a is more complicated; it increases with temperature from 8 to 150 K and then drops abruptly to a finite value between 150 and 200 K.

In absorbing media such as metals and semiconductors, the temperature dependence of a coherent phonon amplitude is often dominated by that of photoexcited carrier density.[16] Figure 3(b) plots the maximum height of the nonoscillatory reflectivity change, A_{el}, as a quantitative measure for photoexcited carrier density. One can immediately notice that the temperature dependence of A_a copies that of A_{el} and conclude that the A_{1g} phonon amplitude is governed by the photoexcited carrier density. However, the temperature dependence of A_e, which decreases to zero above 200 K, cannot be explained by the photoexcited carrier density alone. We will discuss possible explanation in Sec. IV B.

Figure 4(a) shows that the dephasing rates of both phonons increase (i.e., the lifetimes become shorter) at higher temperature. Γ_a in the present study is in a quantitative agreement with the previous time-domain study,[10] where the decay process of the A_{1g} phonon is attributed to the anharmonic decay into two acoustic phonons at Λ point. We note that Γ_e increases much more rapidly with temperature than Γ_a, although the value at 150 K scatters from measurement to measurement. The frequencies of the two phonon modes also show different temperature dependences. While ν_a downshifts clearly with rising temperature, ν_e is almost independent of temperature, exhibiting a very slight upshift up to 120 K. It can be attributed to the large anisotropy in the thermal expansion of Bi,[17] since the nuclear displacements of A_{1g} and E_g modes are perpendicular and parallel to the basal plane, respectively.

Initial phases are very often used as the quick index of the generation mechanism of coherent phonons. It is therefore striking that the coherent A_{1g} and E_g phonons exhibit

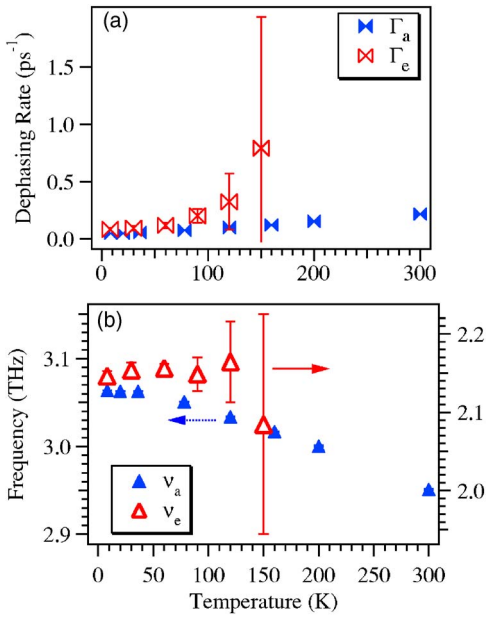

FIG. 4. (Color online) Temperature dependence of (a) the dephasing rates Γ_a and Γ_e and (b) the frequencies ν_a and ν_e of the coherent phonons of Bi. The parameters for the A_{1g} and E_g phonons are obtainedfrom the isotropic and anisotropic reflectivity measurements, respectively. ν_a and ν_e in (b) are plotted to the left and right hand axes, respectively.

clearly different initial phases, as shown in Fig. 5(a). Careful analysis reveals δ_a and δ_e to be $-100° \pm 14°$ and $152° \pm 10°$, respectively. δ_a is close to $-\pi/2$ and consistent with early time-domain studies.[8–10] On the other hand, our phase difference between the two modes, almost $\pi/2$ regardless of temperature [Fig. 5(b)], is noticeably larger than that reported for Sb.[9] If we define solely by δ, our observation would indicate that the dynamics of the A_{1g} mode is purely displacive ($\delta = \pm\pi/2$), while that of the E_g mode is nearly impulsive ($\delta = 0, \pi$). A more unifying model on the generation mechanism will be given in Sec. IV C.

B. Polarization dependence

Figure 6 summarizes A_a and A_e as functions of pump polarization angle θ. The results show that the A_{1g} phonon is isotropic and independent of the pump polarization, while the E_g phonon has $\cos 2\theta$ dependence. Both polarization dependences are in perfect agreement with the expectation from the Raman tensors given in Sec. I. The Raman tensor (2) predicts an isotropic polarization dependence within the xy plane. The tensors (3) are similar to those of GaN[18] and give the scattering cross section depending on θ,

$$S(E_g^{(1)}) \propto d \times \cos(2\theta),$$

$$S(E_g^{(2)}) \propto -d \times \sin(2\theta). \tag{5}$$

The former, whose basis function is x^2-y^2, can be probed with p- or s-polarized probe light, while the latter, with a basis function $-2xy$, with 45°-polarized probe light. Since we employ p-polarized probe in the isotropic measurements and take the difference between the s and p components in the anisotropic measurements, we detect only the $E_g^{(1)}$ in the present study. The good agreement between the observed polarization dependence and the Raman tensors supports that the generations of both coherent phonons are essentially Raman processes.

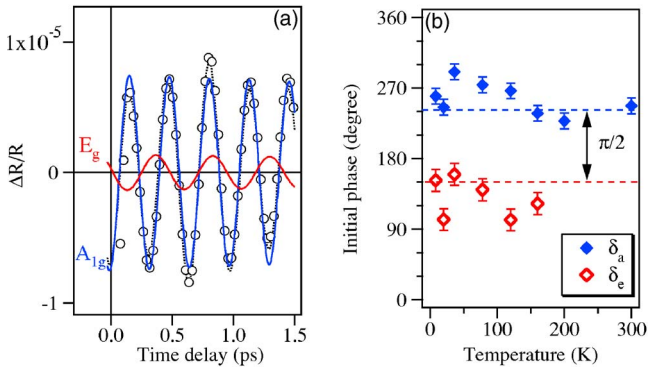

FIG. 5. (Color online) (a) Oscillatory part of the isotropic reflectivity change of Bi at 8 K (open circles), fit to Eq. (4) (dotted curve) and its A_{1g} and E_g components (solid curves). (b) Temperature dependence of the initial phases δ_a and δ_e of the two coherent phonons.

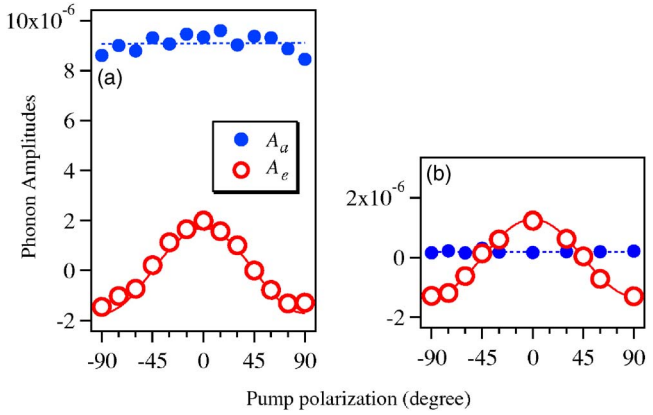

FIG. 6. (Color online) Pump polarization dependence of the initial amplitudes of coherent phonons obtained from (a) isotropic and (b) anisotropic reflectivity changes. Polarization angle is measured from the optical plane. Both measurements are carried out with pump power of 5 mW at 8 K. Solid curves represent fitting with $\cos 2\theta$. Dotted lines are to guide the eyes.

C. Power dependence

Figure 7 summarizes the pump-power dependence of the coherent phonons of Bi at 8 K. A_a and A_e increase linearly with increasing pump power, as shown in Fig. 7(a). We checked the linearity up to mJ/cm^2 pulse energy, above which the coherent phonons start to exhibit a delay-time-dependent frequency shift[12] and amplitude collapse-revival behavior.[15,19] Γ_a and Γ_e are independent of the pump power, as shown in Fig. 7(b), confirming that the decay of the coherent phonons is dominated by the anharmonic coupling[10] rather than the scattering by hot phonons and carriers. The phonon frequencies (not shown in figure) are also independent of the pump power, indicating that the temperature rise under μJ/cm^2 irradiation is negligible at substrate temperature of 8 K. When we increased the pulse energy to mJ/cm^2, both the dephasing rates and the frequencies start to depend dramatically on the pump power.[19]

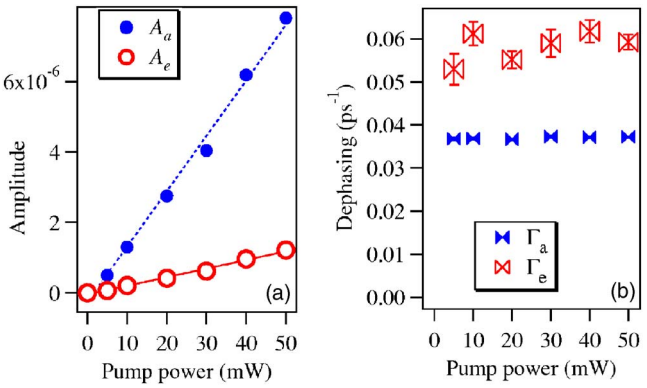

FIG. 7. (Color online) Pump-power dependence of (a) the initial amplitudes and (b) dephasing rates of coherent phonons of Bi obtained from isotropic reflectivity measurement at 8 K.

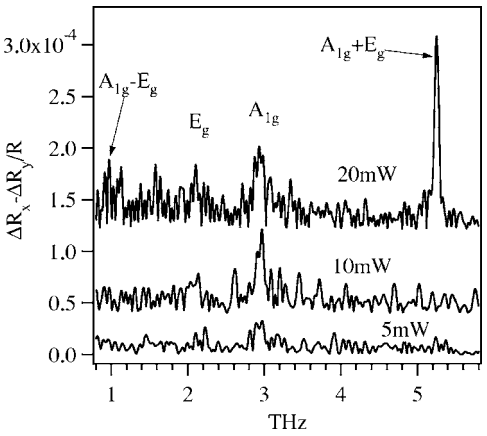

FIG. 8. FT spectra of the oscillatory part of the anisotropic reflectivity change of Bi under different pump powers at room temperature.

The power dependence at room temperature is quite different, as shown in Fig. 8. For pump power of 5 mW, the coherent E_g phonon is negligible, as described in Sec. III A, and the A_{1g} phonon is canceled in anisotropic configuration. With increasing pump power, both the A_{1g} and E_g modes becomes visible. At 20 mW, coherent combination modes ($A_{1g}+E_g$ and $A_{1g}-E_g$) are observed at 5.2 and 0.97 THz, in addition to the fundamentals. Further increase of the pump power leads to irreversible increase of noise in the reflectivity, most probably due to thermal damage on the crystal surface.

The observation of the combination modes at room temperature is in a striking contrast to 8 K, where no combination mode or surface damage is observed up to the maximum power investigated (50 mW or 93 μJ/cm^2). When the pump power is increased above the mJ/cm^2 range, the combination mode is observed even at 8 K.[19] The appearance of the combination modes is a clear sign of enhanced anharmonic coupling between the phonon modes, possibly due to the lattice distortion at temperature close to the melting point. The present results demonstrate that single crystal Bi is easily brought to near melting by a low power laser irradiation at room temperature.

IV. DISCUSSION

A. Temperature dependence of the A_{1g} amplitude

The present study demonstrates that the temperature dependence of the A_{1g} amplitude is dominated solely by that of the electronic amplitude A_{el} or the photoexcited carrier density. A similar strong correlation between the phononic and electronic amplitudes was reported for Zn.[16] Previous time-domain study on polycrystalline Bi also found a rough correlation.[10] We consider this a common feature for absorbing media, in which coherent phonons are driven by the creation of photocarriers, i.e., resonant Raman scattering, field screening, and photo-Dember effect.

The temperature dependence of A_{el} itself is different from material to material. For Zn, both the phononic and electronic amplitudes were decreased monotonically with temperature and fitted by the photoinduced change in the electronic temperature.[16] The same two-temperature model cannot explain the increase of A_{el} (and A_a) with temperature up to 150 K in the present study. We therefore attribute the present result up to 150 K to a slight modification of band structure by thermal expansion.

We find that the drops in A_a, A_e, and A_{el} between 150 and 200 K are irreversible. Heating the sample above 200 K (under laser irradiation) decreases the low-temperature amplitudes by up to 30%. The observed hysteresis indicates that irradiation of 5 mW laser light above 150 K gives a permanent damage. Since the temperature rise under μJ/cm^2 irradiation is estimated to be a few kelvins from the optical penetration depth and the heat capacity, we attribute the drop to a laser-assisted surface modification rather than to the melting of the bulk.

B. Temperature dependence of the E_g amplitude

The observation of all the Raman active modes as coherent phonons and their polarization dependences in the present study fit perfectly the resonant ISRS generation of coherent phonons. It gives a direct evidence that the E_g mode was missing not because of the phonon symmetry but due to some temperature-dependent factor.

The temperature dependence of the E_g amplitude, in contrast to the A_{1g}, does not exhibit a strong correlation with that of the electronic amplitude. It appears, at first glance, as if A_{1g} and E_g are resonantly and nonresonantly generated, respectively. This not only sounds strange in a semimetal, but a resonant Raman study gave a counterevidence; the intensities of the two phonons had exactly the same wavelength dependence in visible and near-infrared regions.[4]

We speculate that the temperature dependence of the E_g amplitude is predominantly determined by the nonlinear enhancement of its damping with temperature, which is demonstrated in Fig. 4(a). It is possible that the vibrational potential of the E_g phonon is more anharmonic than that of the A_{1g} and that the damping of the E_g phonon becomes too fast at 200 K compared with the phonon period (i.e., overdamped). It is an interesting question whether or not the laser-induced surface damage, discussed in Sec. IV A, contributes to the enhancement of the damping of the E_g phonon, since they become conspicuous at the same temperature.

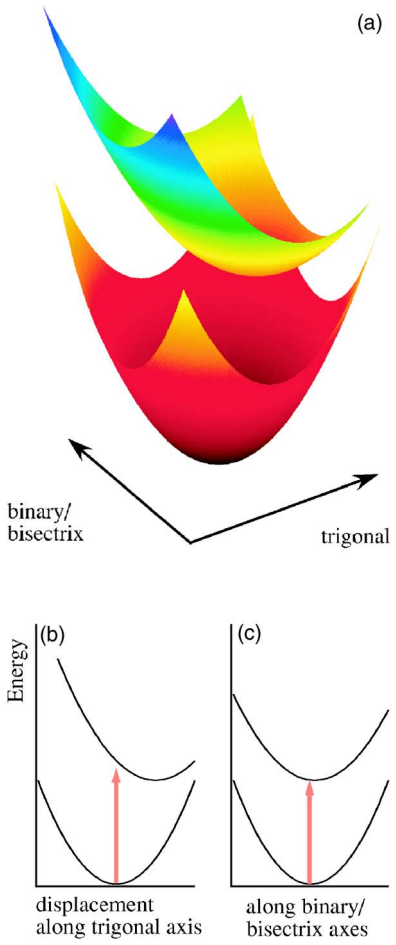

FIG. 9. (Color online) (a) Schematic illustrations of the potential surfaces of ground and excited electronic states and their slices along (b) trigonal and (c) binary/bisectrix axes. Vertical arrows indicate transitions of the nuclei from the ground to the excited energy surface.

C. Initial phase of the coherent oscillations

The present study reveals nearly $\pi/2$ different initial phases between coherent A_{1g} and E_g phonons. It appears, again, to suggest different couplings to the electronic states, DECP and ISRS in the old model[2,8] or resonant and nonresonant ISRSs in the modified one.[11] As already explained in Sec. IV B, however, a resonant Raman study presented an evidence that the two phonons couple to the same electronic transition.[4]

We propose that both the coherent A_{1g} and E_g phonons are generated via a resonant ISRS process and are oscillating on the same excited electronic state, as schematically illustrated in Fig. 9. Here the term *excited* is used in a macroscopic (statistical) sense in which $>10^{18}/\mathrm{cm}^3$ photoexcited carriers occupy nonthermal or hot thermal distribution. It is plausible, though not necessary, that such nonequilibrium carrier distribution can modify the ground-state vibrational potential via electron-phonon coupling.

In this framework, the different initial phases simply indicate whether or not the nonequilibrium carrier distribution shifts the minimum of the potential energy surface along the nuclear displacement in question. The present results mean that the potential is shifted significantly along the trigonal axis, along which the nuclei move in the A_{1g} mode [Fig. 9(b)], but little along the binary and bisectrix axes in the E_g mode [Fig. 9(c)]. Recent first principles calculation on Bi confirmed such an anisotropic shift of the vibrational potential quantitatively.[20]

V. CONCLUSION

In conclusion, we have demonstrated that both the two Raman active phonons in Bi, fully symmetric A_{1g} and doubly degenerated E_g, are excited as coherent phonons at low temperature. The result, together with the polarization dependence, confirms the stimulated Raman generation of the coherent phonons. In contrast to the strong correlation between the A_{1g} phonon and the photoexcited carriers, the amplitude of coherent E_g phonon is rather dominated by the nonlinear enhancement of the damping at high temperature. The initial phases of the two coherent phonons are different by $\pi/2$, indicating that the initial phase is determined by the shift of the vibrational potential minimum between ground and excited electronic states in absorbing media.

ACKNOWLEDGMENTS

This work is partially supported by KAKENHI-16032218 and 17540305 and by Japan-Russia Joint Project No. 05-02-19910.

[1] R. Merlin, Solid State Commun. **102**, 207 (1997).
[2] T. Dekorsy, G. C. Cho, and H. Kurz, in *Light Scattering in Solids VIII*, edited by M. Cardona and G. Güntherodt (Springer, Berlin, 2000), Chap. 4, and references therein.
[3] M. Hase, K. Mizoguchi, H. Harima, S. Nakashima, M. Tani, K. Sakai, and M. Hangyo, Appl. Phys. Lett. **69**, 2474 (1996).
[4] J. B. Rennucci, W. Richter, M. Cardona, and E. Schönherr, Phys. Status Solidi B **60**, 299 (1973).
[5] J. S. Lannin, J. M. Calleja, and M. Cardona, Phys. Rev. B **12**, 585 (1975).
[6] T. K. Cheng, S. D. Brorson, A. S. Kazeroonian, J. S. Moodera, G. Dresselhaus, M. S. Dresselhaus, and E. P. Ippen, Appl. Phys. Lett. **57**, 1004 (1990).
[7] T. K. Cheng, J. Vidal, H. J. Zeiger, G. Dresselhaus, M. S. Dresselhaus, and E. P. Ippen, Appl. Phys. Lett. **59**, 1923 (1991).
[8] H. J. Zeiger, J. Vidal, T. K. Cheng, E. P. Ippen, G. Dresselhaus, and M. S. Dresselhaus, Phys. Rev. B **45**, 768 (1992).
[9] G. A. Garrett, T. F. Albrecht, J. F. Whitaker, and R. Merlin, Phys. Rev. Lett. **77**, 3661 (1996).
[10] M. Hase, K. Mizoguchi, H. Harima, S. Nakashima, and K. Sakai, Phys. Rev. B **58**, 5448 (1998).
[11] T. E. Stevens, J. Kuhl, and R. Merlin, Phys. Rev. B **65**, 144304 (2002).
[12] M. Hase, M. Kitajima, S. Nakashima, and K. Mizoguchi, Phys. Rev. Lett. **88**, 067401 (2002); **93**, 109702 (2004).
[13] S. Fahy and D. A. Reis, Phys. Rev. Lett. **93**, 109701 (2004).
[14] E. D. Murray, D. M. Frits, J. K. Wahlstrand, S. Fahy, and D. A. Reis, Phys. Rev. B **72**, 060301(R) (2005).
[15] O. V. Misochko, M. Hase, K. Ishioka, and M. Kitajima, Phys. Rev. Lett. **92**, 197401 (2004); Phys. Lett. A **321**, 381 (2004).
[16] M. Hase, K. Ishioka, J. Demsar, K. Ushida, and M. Kitajima, Phys. Rev. B **71**, 184301 (2005).
[17] G. K. White, J. Phys. C **2**, 575 (1969).
[18] K. J. Yee, K. G. Lee, E. Oh, D. S. Kim, and Y. S. Lim, Phys. Rev. Lett. **88**, 105501 (2002).
[19] O. V. Misochko, K. Ishioka, M. Hase, and M. Kitajima (unpublished).
[20] E. S. Zijlstra, L. I. Tatarinova, and M. E. Garcia (unpublished).